

Nonreciprocal charge current in a bulk Rashba semiconductor above the band crossing point

Aniruddha Pan  and D. C. Marinescu 

Department of Physics and Astronomy, Clemson University, Clemson, South Carolina 29634, USA



(Received 25 March 2022; revised 16 May 2022; accepted 13 October 2022; published 25 October 2022)

We calculate the nonreciprocal charge current in a bulk semiconductor with Rashba spin-orbit coupling subjected to crossed electric and magnetic fields. By using a second-order distribution function derived in a perturbative approach that considers the change in the local electron energy induced by the electric field, we find that, in contrast with previous theoretical estimates, a charge current proportional to the applied magnetic field exists for all values of the chemical potential, above or below the band crossing point (BCP), the energy where the two chiral conduction bands intersect. The persistence of the quadratic electric current across the BCP is a consequence of the chiral dependence of the relaxation times, an effect neglected before.

DOI: [10.1103/PhysRevB.106.165308](https://doi.org/10.1103/PhysRevB.106.165308)

I. INTRODUCTION

After being at the center of many theoretical and experimental investigations of magnetic and transport phenomena in two-dimensional zinc-blende quantum wells with inversion asymmetry [1,2], the Rashba interaction [3] has been more recently playing a prominent role in new, interesting physics occurring in three-dimensional systems. In these materials, inversion asymmetry along the c axis creates a large Rashba coupling between the electron momentum and its spin in the plane perpendicular to the axis that dominates the observed phenomenology in many experimental settings [4–7].

One of the most important experimental manifestations of the inversion symmetry breaking in these systems is the existence of the nonreciprocal charge transport, characterized by different rightward- and leftward-propagating currents [8]. Systems that support this unidirectional effect are currently being considered for potential application of unidirectional magnetoresistance in the absence of a ferromagnetic layer.

In the presence of crossed electric and magnetic fields, say E_x and B_y , the nonreciprocal resistance R_{nr} is given by [9,10],

$$R_{\text{nr}}(I, B) = \gamma R_0 I_x B_y, \quad (1)$$

where R_0 is the resistance at zero magnetic field and I_x is the electric current along the \hat{x} direction. This result represents the first-order correction to Ohm's law, which takes into account an expression for the electric current in a conductor of cross section A of the form $I = j_x A = A(\sigma_1 E_x + \sigma_2 E_x^2)$. σ_1 and σ_2 are the linear and quadratic conductivities, the existence of the latter being conditioned by the application of a magnetic field along a perpendicular direction. This is easy to understand considering that the magnetic field which couples with a spin along the same direction through the Zeeman interaction, shifts the momentum in the orthogonal direction on account of the spin-orbit interaction. Depending on the direction of I_x , R_{nr} can be positive or negative, thus increasing or decreasing the overall resistance.

The coefficient of nonreciprocity γ is expressed in terms of σ_1 and σ_2 as

$$\gamma = -\frac{1}{AB_y} \frac{\sigma_2}{(\sigma_1)^2}. \quad (2)$$

The topic of the nonreciprocal current was revisited more recently in connection with the inversion symmetry breaking in systems with large spin-orbit coupling, such as bulk-Rasha semiconductors. The existence of the currents and their dependence on the electric and magnetic fields in agreement with Eq. (1) was confirmed experimentally in BiTeBr [10] and in room-temperature α -GeTe [11]. In both cases, the experiments were done in the transport regime corresponding to an equivalent two-dimensional (2D) potential μ below the band crossing point (BCP), the energy value that designates the intersection of the 2D chiral conductivity bands at zero momentum, $\mathbf{p} = 0$.

The theoretical estimate of σ_2 that determines the coefficient γ , presented in the same references, indicated that a second-order charge current exists only for a chemical potential μ below BCP. For μ above BCP, the nonlinear charge current simply disappears generating a step-like discontinuity around BCP. In Ref. [11] it was further posited that this discontinuity diminishes at finite temperatures, even though below BCP σ_2 is temperature independent.

The discontinuity in σ_2 is surprising considering that all the other variables in this problem, such as electron velocities, single-particle energies, and the linear conductivity σ_1 are continuous functions of the chemical potential. Although the result was attributed to the existence of two Fermi surfaces with opposite helicities above BCP [10,11], the cancellation remains a mathematically disturbing event since a response function such as a conductivity should be continuous.

σ_2 is calculated straightforwardly in a semi-classical transport theory that sums the velocities of each state multiplied by a corresponding distribution function quadratic in the electric field. In Refs. [10,11], calculations were performed using a second-order distribution function derived iteratively from the

Boltzmann transport equation, $\delta f_{it}^{(2)}(\mathbf{p}) = (e\tau \mathbf{E} \cdot \nabla_{\mathbf{p}})^2 f^0(\epsilon_{\mathbf{p}})$, where f^0 is the equilibrium Fermi distribution function of an electron of momentum \mathbf{p} and τ is the relaxation time.

In this paper we propose an alternative calculation that uses a second-order distribution function derived in an approximation that considers the change in the local energy of the particle, $\delta f^{(2)}(\epsilon_{\mathbf{p}}) = \frac{1}{2}(e\mathbf{E} \cdot \mathbf{v}_{\mathbf{p}}\tau)^2 \left(\frac{d^2 f^0}{d\epsilon_{\mathbf{p}}^2}\right)$ [12], where $\mathbf{v}_{\mathbf{p}}$ is the electron velocity. This choice is motivated by the observation that the iterative solution $\delta f_{it}^{(2)}$ does not satisfy self-consistently the collision term of the Boltzmann transport equation, and in this sense it is not correct. Moreover, for μ above the BCP, it diverges at the origin in the momentum space, a technical difficulty that precludes the incorporation in the second-order current calculation of a multiband relaxation time whose chiral-dependent part would select exactly the divergent terms. Here we show that it is precisely this previously neglected feature of the problem that guarantees the continuity of σ_2 across BCP.

II. HAMILTONIAN

A conduction electron of momentum $\mathbf{p} = \{p_x, p_y, p_z\}$ and spin $\sigma = \{\sigma_x, \sigma_y, \sigma_z\}$ in a bulk Rashba semiconductor placed in a magnetic field $\mathbf{B} = (0, B_y, 0)$ is described by a Hamiltonian [10]

$$H_0 = \frac{p_z^2}{2m_{\parallel}} + \frac{p_x^2 + p_y^2}{2m_{\perp}} + \alpha(p_x\sigma_y - p_y\sigma_x) - B_y\sigma_y, \quad (3)$$

where m_{\parallel} and m_{\perp} are the effective masses along the \hat{z} axis and in the \hat{x} - \hat{y} plane, while B_y is a contracted notation for the Zeeman splitting, $g\mu_B B_y\sigma_y/2$ with μ_B the Bohr magneton and g the effective gyromagnetic factor. α is the Rashba coupling constant. $m_{\perp}\alpha^2/2$ can range in value from several meVs like in the zinc-blende quantum well structures to tens of meV bulk polar semiconductors. In the following considerations, it is assumed that the spin-orbit coupling is the dominant interaction in comparison with the Zeeman splitting, $m_{\perp}\alpha^2/2 \gg B_y$.

A unitary transformation $p_x \rightarrow p_x - B_y/\alpha$, $p_y \rightarrow p_y$, $p_z \rightarrow p_z$ modifies the Hamiltonian to

$$H = \frac{p_z^2}{2m_{\parallel}} + \frac{1}{2m_{\perp}} \left(p_x - \frac{B_y}{\alpha}\right)^2 + \frac{p_y^2}{2m_{\perp}} + \alpha(p_x\sigma_y - p_y\sigma_x), \quad (4)$$

a form which permits an exact diagonalization in the spin space. (There is no loss of generality in this problem in choosing only a B_y magnetic field. An in-plane magnetic field of arbitrary direction, with nonzero components B_x and B_y shifts both momenta to $p_x - B_y/\alpha$ and $p_y + B_x/\alpha$. The calculation of the electric currents, obtained by summing the momenta along the x and y directions proceeds in an identical fashion.)

Since the momenta along the three coordinate axes are good quantum numbers, in the following considerations we replace the corresponding operator in the expression of the Hamiltonian by its eigenvalue. The single-particle energies are obtained as

$$\mathcal{E}_{\xi} = \frac{p_z^2}{2m_{\parallel}} + \frac{1}{2m_{\perp}} \left(p_x - \frac{B_y}{\alpha}\right)^2 + \frac{p_y^2}{2m_{\perp}} + \xi\alpha p, \quad (5)$$

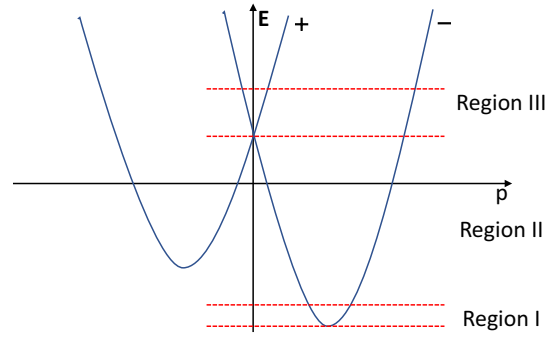


FIG. 1. The energy spectrum of the Rashba system. The three marked regions determine the particulars of the transport phenomenology as a function of the chemical potential μ .

where $p = \sqrt{p_x^2 + p_y^2}$ and $\xi = \pm 1$. The eigenfunctions, normalized to a volume V , are

$$|u_{+}\rangle = \frac{e^{i\mathbf{p}\cdot\mathbf{r}}}{\sqrt{2V}} \begin{pmatrix} 1 \\ -ie^{i\varphi} \end{pmatrix}, \quad |u_{-}\rangle = \frac{e^{i\mathbf{p}\cdot\mathbf{r}}}{\sqrt{2V}} \begin{pmatrix} -ie^{-i\varphi} \\ 1 \end{pmatrix}, \quad (6)$$

where $\tan \varphi = -p_x/p_y$.

Since the interesting physics in this problem concerns the \hat{x} - \hat{y} dynamics, we eliminate the energy associated with the longitudinal direction and write $\epsilon_{\xi} = \mathcal{E}_{\xi} - p_z^2/2m_{\parallel}$. The two-dimensional energy spectrum is therefore written as

$$\epsilon_{\xi} = \frac{1}{2m_{\perp}} \left(p + \xi m\alpha + \frac{B_y}{\alpha} \cos \varphi\right)^2 + \frac{B_y^2}{2m_{\perp}\alpha^2} - \frac{1}{2m_{\perp}} \left(\frac{B_y}{\alpha} \cos \varphi + m_{\perp}\xi\alpha\right)^2. \quad (7)$$

These equations describe two paraboloids centered at

$$p_{\text{center}} = -\xi m_{\perp}\alpha - \frac{B_y}{\alpha} \cos \varphi, \quad (8)$$

of minima

$$\epsilon_{\min,\xi} = \frac{B_y^2}{2m_{\perp}\alpha^2} \sin^2 \varphi - \frac{m_{\perp}\alpha^2}{2} - \xi B_y \cos \varphi, \quad (9)$$

as shown schematically in Fig. 1

The two Fermi surfaces intersect at $\mathbf{p} = 0$, when $E_{\text{BCP}} = \frac{B_y^2}{2m_{\perp}\alpha^2}$. This energy value denotes the band crossing point (BCP) [11] or the Dirac point in Ref. [18]. In the following considerations, we shift the origin of the 2D energy at this value.

The Fermi momenta are calculated from $\epsilon_{\xi} = \mu$, where μ is the effective 2D chemical potential obtained from the true three-dimensional (3D) potential by subtracting the kinetic energy along the c axis. Since the Fermi momenta are positively defined, for energies below the BCP, they are determined exclusively by the $\xi = -1$ paraboloid's intersection with the constant μ plane as shown in Fig. 1.

The position of the chemical potential determines the various dynamic regimes of this problem. Following the well-established discussion lines [10,11], we differentiate three regions.

Regions I and II correspond to chemical potential values below BCP, i.e., $\mu < 0$. In region I μ satisfies

$$-\frac{m\alpha^2}{2} - B_y \leq \mu \leq -\frac{m\alpha^2}{2} + B_y. \quad (10)$$

In this situation, the Fermi surface $\xi = -1$ is not totally enclosed, the angular distribution of the electron states being limited to the interval $[\varphi_{\min}, 2\pi - \varphi_{\min}]$, where

$$\varphi_{\min} = \arccos \frac{\frac{m_{\perp}\alpha^2}{2} + \mu}{B_y}, \quad (11)$$

a result obtained from a linear approximation in the magnetic field of Eq. (9).

The corresponding Fermi momenta for $\eta = \pm 1$ are given by

$$p_{\pm}^{\eta} = m_{\perp}\alpha - \frac{B_y}{\alpha} \cos \varphi + \eta \sqrt{2m_{\perp}\mu + \left(\frac{B_y}{\alpha} \cos \varphi - m_{\perp}\alpha\right)^2}. \quad (12)$$

Region II is reached when the chemical potential satisfies

$$-\frac{m_{\perp}\alpha^2}{2} + B_y \leq \mu \leq 0, \quad (13)$$

indicating that the $\xi = -1$ Fermi surface is completely encircled. Therefore, $\varphi \in [0, 2\pi]$. The Fermi momenta are the same as in Eq. (12).

In region III the chemical potential is above the BCP, $\mu > 0$ and both Fermi surfaces for $\xi = \pm 1$ participate in transport with Fermi momenta

$$p_{\xi} = \sqrt{2m_{\perp}\mu + \left(\frac{B_y}{\alpha} \cos \varphi + \xi m_{\perp}\alpha\right)^2} - \xi m_{\perp}\alpha - \frac{B_y}{\alpha} \cos \varphi. \quad (14)$$

Since the energy width of region I is of the order B_y , much smaller than $m_{\perp}\alpha^2/2$, in the following considerations we will neglect it and refer only to the region below the BCP (region II) and the region above the BCP (region III).

III. TRANSPORT FORMALISM

In the presence of an electric field, the electron distribution function $f_{\mathbf{p}}$ satisfies

$$\dot{\mathbf{p}} \cdot \nabla_{\mathbf{p}} f_{\mathbf{p}} = \left(\frac{\partial f_{\mathbf{p}}}{\partial t} \right)_{\text{coll}}. \quad (15)$$

With $\dot{\mathbf{p}} = -e\mathbf{E}$, the first-order correction is obtained by applying the derivative $\nabla_{\mathbf{p}}$ to the equilibrium Fermi distribution function written for energy $\epsilon_{\mathbf{p}}$, $f^0(\epsilon_{\mathbf{p}}) = [e^{\beta(\epsilon_{\mathbf{p}} - \mu)} + 1]^{-1}$. The collision integral in Eq. (15) is calculated using a linear solution of the type $\delta f_{\mathbf{p}}^{(1)} = C(\epsilon_{\mathbf{p}}) \nabla_{\mathbf{p}} \epsilon_{\mathbf{p}} \cdot \mathbf{E} (-df^0/d\epsilon_{\mathbf{p}})$ and the result is expressed in terms of a relaxation time τ ,

$$\left(\frac{\partial f_{\mathbf{p}}}{\partial t} \right)_{\text{coll}} = -\frac{\delta f_{\mathbf{p}}^{(1)}}{\tau}. \quad (16)$$

The first-order solution to the Boltzmann transport equation (BTE) is therefore [13]

$$\delta f_{\mathbf{p}}^{(1)} = e\tau \mathbf{v}_{\mathbf{p}} \cdot \mathbf{E} \frac{df^0}{d\epsilon}, \quad (17)$$

where $\mathbf{v}_{\mathbf{p}} = \nabla_{\mathbf{p}} \epsilon_{\mathbf{p}}$ is the electron velocity.

To obtain the second-order distribution function, an iterative algorithm based on the BTE was proposed in Ref. [14] and subsequently used in many applications that dealt with nonlinear transport effects, including the nonreciprocal current problem [10,11,15]. In this approach, $\delta f_{\mathbf{p}}^{(2)} = (e\tau \mathbf{E} \cdot \nabla_{\mathbf{p}})^2 f_{\mathbf{p}}^0$. In Ref. [12] we showed that this result violated the linearity premise underlying the relaxation time approximation of the collision integral. Consequently, we suggested a different procedure for generating the second-order distribution function in a semi-classical approximation, based on the local perturbation of the single-particle distribution function induced by the external fields. Thus, the addition of an electrostatic potential $V(\mathbf{r}) = -\mathbf{E} \cdot \mathbf{r}$, modifies locally the electron energy to $\tilde{\epsilon}_{\mathbf{p}} = \epsilon_{\mathbf{p}} + e\mathbf{E} \cdot \mathbf{r}$, a change considered weak in respect to the Fermi energy. The electron distribution function is just the Fermi function written for the local energy

$$\tilde{f}_{\mathbf{p}}(\mathbf{r}) = \left\{ 1 + \exp \left[\frac{\epsilon_{\mathbf{p}} - \epsilon_F + e\mathbf{E} \cdot \mathbf{r}}{k_B T} \right] \right\}^{-1}. \quad (18)$$

Equation (18) can be expanded in a series of terms proportional to powers of the electric field. When the linear terms are constrained to replicate the solution of the BTE, it is found that $\mathbf{r} = \mathbf{v}_{\mathbf{p}} \tau$, a result which establishes the spatial range of the approximation. τ is the relaxation time obtained in the Boltzmann approximation, given by

$$\frac{\hbar}{\tau} = v_0 \int |V_{\mathbf{p},\mathbf{p}'}|^2 (1 - \cos \theta_{\mathbf{p}\mathbf{p}'}) d\theta_{\mathbf{p}\mathbf{p}'}, \quad (19)$$

with v_0 the density of states at the Fermi surface and $|V_{\mathbf{p},\mathbf{p}'}|^2$ is the scattering matrix element of an electron of initial and final momenta, \mathbf{p} and \mathbf{p}' , respectively.

With this, the second-order distribution function becomes

$$\delta f_{\mathbf{p}}^{(2)} = \frac{1}{2k_B T} (e\tau \mathbf{E} \cdot \mathbf{v}_{\mathbf{p}})^2 \tanh \frac{\epsilon_{\mathbf{p}} - \epsilon_F}{2k_B T} \left(-\frac{\partial f_{\mathbf{p}}^0}{\partial \epsilon_{\mathbf{p}}} \right). \quad (20)$$

As we show below, using Eq. (20) to evaluate the nonreciprocal current is a key step in recovering the continuity of quadratic conductivity across BCP.

For an electric field parallel to the \hat{x} axis, the electron velocity v_x is, from Eq. (7),

$$v_x = \left(\frac{p_x}{m_{\perp}} + \frac{B_y}{\alpha} \right) + \xi \alpha p_x / p. \quad (21)$$

It is useful to express the velocity as a function of the chemical potential since, in the end, these values will enter the calculation. Consequently, below the BCP the velocity is, from Eq. (7), written for $\xi = -1$,

$$v_{x\eta} = \eta \frac{1}{m_{\perp}} \sqrt{2m_{\perp}\mu + \left(\frac{B_y}{\alpha} \cos \varphi - m_{\perp}\alpha\right)^2} \times \cos \varphi + \frac{B_y}{m_{\perp}\alpha} \sin^2 \varphi. \quad (22)$$

Above the BCP, from Eqs. (7), (21), and (14), the velocity is

$$v_{x\xi} = \frac{1}{m_{\perp}} \sqrt{2m_{\perp}\mu + \left(\frac{B_y}{\alpha} \cos \varphi + \xi m_{\perp}\alpha\right)^2} \times \cos \varphi + \frac{B_y}{m_{\perp}\alpha} \sin^2 \varphi. \quad (23)$$

To round up the general presentation of the transport formalism, we introduce the chiral-dependent relaxation times obtained by generalizing the relaxation time calculation [13] to a two-band conduction regime in a system with Rashba interaction as discussed in Refs. [16,17] whose approach we adapt to a two dimensional system. (Even though below BCP there is only one Fermi surface associated with $\xi = -1$ because the electron velocity at the Fermi level is $\eta = \pm 1$ dependent, two different relaxation times are involved). We anticipate that their inclusion in the calculation is essential in this problem.

Thus, in first order in α , for a chiral index λ (ξ above BCP and $-\eta$ below BCP), the relaxation time Eq. (19) becomes

$$\frac{\hbar}{\tau_{\lambda}} = \frac{\hbar}{\tau} \left(1 + \lambda \frac{m_{\perp}\alpha}{2p_0}\right), \quad (24)$$

with

$$p_0 = \sqrt{(m_{\perp}\alpha)^2 + 2m_{\perp}\mu}. \quad (25)$$

We anticipate that the proper consideration of the chiral effect on the relaxation time does not have any effect on the linear conductivity calculation, while it is essential in obtaining a correct value for the quadratic term σ_2 .

IV. CHARGE CURRENTS

A. Linear charge currents

The first-order current below BCP is calculated from Eqs. (12), (17), and (22),

$$\begin{aligned} j_{x,<}^{(1)} &= -e \sum_{p \in [p^-, p^{\pm}]} v_{x\eta} \delta f_{\mathbf{p}}^{(1)} \\ &= \frac{(e^2 E_x)}{(2\pi \hbar)^2} \sum_{\eta=\pm 1} \eta \tau_{\eta} \int_0^{2\pi} \left[v_{x\eta}^2 p_{\eta}^{\eta} \frac{dp_{\eta}^{\eta}}{d\epsilon} \right]_{\mu} d\varphi \\ &= \frac{e^2 E_x \tau}{2\pi \hbar^2} \alpha \sqrt{(m_{\perp}\alpha)^2 + 2m_{\perp}\mu}. \end{aligned} \quad (26)$$

Here $\sum_{p \in [p^-, p^{\pm}]} \rightarrow \sum_{\eta=\pm 1} \eta$.

Above the BCP, currents are evaluated using Eqs. (23) and (14)

$$\begin{aligned} j_{x,>}^{(1)} &= -e \sum_{\xi=\pm 1} \sum_{\mathbf{p}} v_{x\xi} \delta f_{\mathbf{p}}^{(1)} \\ &= \frac{e^2 E_x}{(2\pi \hbar)^2} \sum_{\xi=\pm 1} \tau_{\xi} \int_0^{2\pi} d\varphi \int_0^{\infty} \left[v_{x\xi}^2 p_{\xi} \frac{dp_{\xi}}{d\epsilon} \right] \left(-\frac{df^0}{d\epsilon} \right) d\epsilon \\ &= \frac{e^2 E_x}{(2\pi \hbar)^2} \sum_{\xi} \tau_{\xi} \int_0^{2\pi} \left[v_{x\xi}^2 p_{\xi} \frac{dp_{\xi}}{d\epsilon} \right]_{\mu} d\varphi \\ &= \frac{e^2 E_x \tau}{2\pi \hbar^2 m_{\perp}} [(m_{\perp}\alpha)^2 + 2m_{\perp}\mu]. \end{aligned} \quad (27)$$

From Eqs. (26) and (27), we determine the linear conductivities

$$\sigma_1 = \begin{cases} \frac{e^2 \tau}{2\pi \hbar^2} \alpha \sqrt{(m_{\perp}\alpha)^2 + 2m_{\perp}\mu}, & \mu < 0, \\ \frac{e^2 \tau}{2\pi \hbar^2 m_{\perp}} [(m_{\perp}\alpha)^2 + 2m_{\perp}\mu], & \mu > 0. \end{cases} \quad (28)$$

As expected there are no first-order contributions in the magnetic field and σ_1 is continuous across BCP.

B. Bilinear electric currents

The nonreciprocal currents E_x and linear in B_y are now calculated using the second-order distribution function Eq. (20). Because $\delta f_{\mathbf{p}}^{(2)}$ is proportional with $\tanh[(\epsilon_{\mathbf{p}} - \mu)/2k_B T]$ which cancels at μ , the summation algorithm uses the Sommerfeld expansion [13].

Below the BCP is computed with input from Eqs. (22) and (12). In the final steps of the calculation we linearize the results in the magnetic field and introduce p_0 from Eq. (25). Thus,

$$\begin{aligned} j_{x,<}^{(2)} &= -e \sum_{p \in [p^-, p^{\pm}]} v_{x\eta} \delta f_{\mathbf{p}}^{(2)} \\ &= \frac{-e^3 E_x^2}{48 \hbar^2} \sum_{\eta} \eta \tau_{\eta}^2 \int_0^{2\pi} \frac{d}{d\epsilon} \left[\left(p_{\eta}^{\eta} \frac{dp_{\eta}^{\eta}}{d\epsilon} v_x^3 \right) \right]_{\mu} d\varphi \\ &= \frac{-e^3 E_x^2}{48 \hbar^2} \sum_{\eta} \tau_{\eta}^2 \int_0^{2\pi} \left[3 \frac{p_0}{m_{\perp}} \cos^3 \varphi + 2\eta \alpha \cos^3 \varphi \right. \\ &\quad \left. - \frac{B_y}{p_0} (\cos^4 \varphi - \sin^2 \varphi \cos^2 \varphi) \right. \\ &\quad \left. - 2\eta \frac{B_y}{m_{\perp}\alpha} (\cos^4 \varphi - 3 \sin^2 \varphi \cos^2 \varphi) \right] d\varphi \\ &= \frac{\pi e^3 \tau^2 E_x^2}{16 \hbar^2} \frac{B_y}{\sqrt{(m_{\perp}\alpha)^2 + 2m_{\perp}\mu}}. \end{aligned} \quad (29)$$

The result in Eq. (29) has the same energy dependence as in Refs. [10,11], but differs slightly in magnitude, with a leading numerical prefactor of $\pi/16 = 0.2$ versus $3/8\pi = 0.12$ in Refs. [10,11]. On account of the angular integral effectively canceling all the η -dependent terms in the current kernel, the chiral component of the relaxation time does not affect the final result. This situation changes dramatically for μ above BCP, when considering chiral-dependent relaxation times is essential in preserving the continuity of the charge current.

When $\mu > 0$, the nonreciprocal current is evaluated from Eqs. (23), (14), and (25),

$$\begin{aligned} j_{x,>}^{(2)} &= -e \sum_{\mathbf{p}, \xi} v_{x\xi} \delta f_{\mathbf{p}}^{(2)} \\ &= -\frac{e^3 E_x^2}{48 \hbar^2} \sum_{\xi} \tau_{\xi}^2 \int_0^{2\pi} \frac{d}{d\epsilon} \left[p_{\xi} \frac{dp_{\xi}}{d\epsilon} v_{x\xi}^3 \right]_{\mu} d\varphi \\ &= -\frac{e^3 E_x^2}{48 \hbar^2} \sum_{\xi} \tau_{\xi}^2 \int_0^{2\pi} \left[3 \frac{p_0}{m_{\perp}} \cos^3 \varphi - 2\xi \alpha \cos^3 \varphi \right. \end{aligned}$$

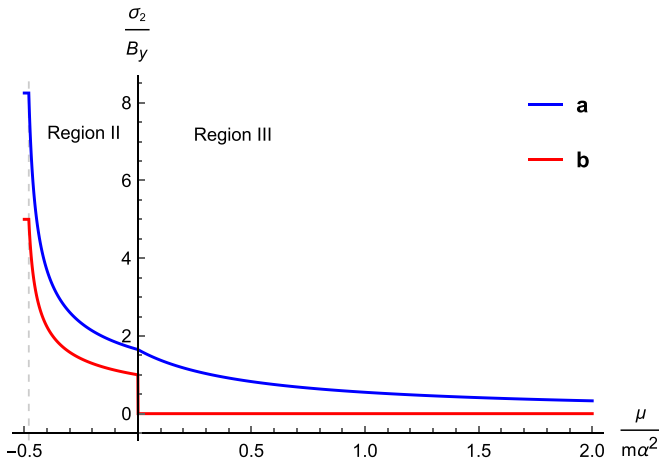


FIG. 2. The 2D second-order conductivity in Eq. (31) (a) is compared with the result of Ref. [10] (b). Continuity across the $\mu = 0$ point replaces the step function discontinuity.

$$\begin{aligned}
 & + 3\xi \frac{B_y}{p_0} (\cos^4 \varphi - \sin^2 \varphi \cos^2 \varphi) \\
 & + 2 \frac{B_y}{m_{\perp} \alpha} (3 \sin^2 \varphi \cos^2 \varphi - \cos^4 \varphi) \Big] d\varphi \\
 & = -\frac{\pi e^3 E_x^2 B_y}{32 \hbar^2 p_0} \sum_{\xi} \xi \left(1 - \xi \frac{m_{\perp} \alpha}{p_0} \right) \\
 & = \frac{\pi e^3 \tau^2 E_x^2}{16 \hbar^2} \frac{m_{\perp} \alpha B_y}{(m_{\perp} \alpha)^2 + 2m_{\perp} \mu}. \quad (30)
 \end{aligned}$$

In the second to last line of Eq. (30), the linearized (in $m_{\perp} \alpha/p_0$) expression of $\tau_{\xi}^{(2)}$ was introduced from Eq. (24).

Thus, the quadratic conductivities are

$$\sigma_2 = \begin{cases} \frac{\pi e^3 \tau^2}{16 \hbar^2} \frac{B_y}{\sqrt{(m_{\perp} \alpha)^2 + 2m_{\perp} \mu}}, & \mu < 0, \\ \frac{\pi e^3 \tau^2}{16 \hbar^2} \frac{m_{\perp} \alpha B_y}{(m_{\perp} \alpha)^2 + 2m_{\perp} \mu}, & \mu > 0. \end{cases} \quad (31)$$

In the limit of $\mu \rightarrow 0$, σ_2 is continuous across BCP. Essential for this result is the presence of the chiral correction to the relaxation time. Otherwise, $j_{x>BCP}^{(2)}$ would be zero, the result of Refs. [10,11]. Incorporating these relaxation times in a formalism based on the iterative solution for $\delta f_{\mathbf{p}}^{(2)}$ is impossible because that function exhibits a divergence at $p = 0$ that would couple exactly into the chiral dependence of the times leading to an overall divergent result. In Fig. 2 we compare the two expressions for the second-order conductivity in the second and third regions.

From Eqs. (28) and (31) a general expression can be introduced for the quadratic conductivity in terms of the linear conductivity

$$\sigma_2 = \frac{e^5 \tau^3}{32 \hbar^4} \frac{\alpha}{\sigma_1} B_y, \quad (32)$$

while a corresponding coefficient of nonreciprocity results from Eq. (2)

$$\gamma = -\frac{1}{A} \frac{e^5 \tau^3}{32 \hbar^4} \frac{\alpha}{\sigma_1^3}. \quad (33)$$

V. CONCLUSION

Using a quadratic distribution function derived in a local energy approximation, $\delta f^{(2)}(\epsilon_{\mathbf{p}})$ in Eq. (20), we calculated the second-order charge current in a Rashba semiconductor under crossed electric and magnetic fields. While a uniband relaxation time suffices for calculating σ_2 below the BCP since no additional contributions to the current arise from the chiral corrections, considering a chiral-dependent relaxation rate is essential for assuring the continuity of σ_2 . The nonreciprocal current above BCP decreases with μ and is independent of temperature, another characteristic feature of a totally degenerate system. Although we chose not to undergo the calculation here, σ_2 can be evaluated analytically in region I as well by using the same general algorithm used in calculating the current below BPC, but with a modified angular range $\varphi \in [\varphi_{\min}, 2\pi - \varphi_{\min}]$, where φ_{\min} is given in Eq. (11)

The rectification current is thus expected to occur in all noncentrosymmetric semiconductors with spin-orbit interaction in the presence of crossed electric and magnetic fields, regardless of the position of the effective 2D chemical potential μ relative to BCP. Since this is determined by the electron concentration (doping level), the number of favorable situations can be quite big. Prime candidates for observing this phenomenon are zinc-blende quantum wells with Rashba-Dresselhaus coupling, where the 2D chemical potential is always positive. Further, polar Rashba semiconductors like those used in Refs. [10,11] can be driven in a regime with positive μ . Experimentally, this situation was already realized in BiTeI in Ref. [18] where samples with $n = 4.6 \times 10^{18} \text{ cm}^{-3}$ and $n = 8.3 \times 10^{18} \text{ cm}^{-3}$ were found to have an effective 2D chemical potential below BCP, while those with $n = 4.2 \times 10^{19} \text{ cm}^{-3}$ and $n = 6.7 \times 10^{19} \text{ cm}^{-3}$ had a μ above BCP. Similarly, this effect should also be detected in the surface Weyl states of 3D topological insulators, as discussed in Ref. [15] where the effective 2D chemical potential can be driven through doping above the band crossing point.

- [1] J. Sinova, S. O. Valenzuela, J. Wunderlich, C. H. Back, and T. Jungwirth, Spin Hall effects, *Rev. Mod. Phys.* **87**, 1213 (2015).
- [2] A. Manchon, H. C. Koo, J. Nitta, S. M. Frolov, and R. A. Duine, New perspectives for Rashba spin-orbit coupling, *Nat. Mater.* **14**, 871 (2015).
- [3] Y. Bychkov and E. I. Rashba, *JETP Lett.* **39**, 78 (1984).
- [4] K. Ishizaka, M. S. Bahramy, H. Murakawa, M. Sakano, T. Shimojima, T. Sonobe, K. Koizumi, S. Shin, H. Miyahara, A.

- Kimura, K. Miyamoto, T. Okuda, H. Namatame, M. Taniguchi, R. Arita, N. Nagaosa, K. Kobayashi, Y. Murakami, R. Kumai, Y. Kaneko *et al.*, Giant Rashba-type spin splitting in bulk BiTeI, *Nat. Mater.* **10**, 521 (2011).

- [5] J. S. Lee, G. A. H. Schober, M. S. Bahramy, H. Murakawa, Y. Onose, R. Arita, N. Nagaosa, and Y. Tokura, Optical Response of Relativistic Electrons in the Polar BiTeI Semiconductor, *Phys. Rev. Lett.* **107**, 117401 (2011).

- [6] C. Martin, A. V. Suslov, S. Buvaev, A. F. Hebard, P. Bugnon, H. Berger, A. Magrez, and D. B. Tanner, Experimental determination of the bulk Rashba parameters in BiTeBr, *Europhys. Lett.* **116**, 57003 (2016).
- [7] J. Krempaský, H. Volfová, S. Muff, N. Pilet, G. Landolt, M. Radović, M. Shi, D. Kriegner, V. Holý, J. Braun, H. Ebert, F. Bisti, V. A. Rogalev, V. N. Strocov, G. Springholz, J. Minár, and J. H. Dil, Disentangling bulk and surface Rashba effects in ferroelectric α -GeTe, *Phys. Rev. B* **94**, 205111 (2016).
- [8] R. Wakatsuki and N. Nagaosa, Nonreciprocal Current in Noncentrosymmetric Rashba Superconductors, *Phys. Rev. Lett.* **121**, 026601 (2018).
- [9] G. L. J. A. Rikken and P. Wyder, Magnetoelectric Anisotropy in Diffusive Transport, *Phys. Rev. Lett.* **94**, 016601 (2005).
- [10] T. Ideue, K. Hamamoto, S. Koshikawa, M. Ezawa, S. Shimizu, Y. Kaneko, Y. Tokura, N. Nagaosa, and Y. Iwasa, Bulk rectification effect in a polar semiconductor, *Nat. Phys.* **13**, 578 (2017).
- [11] Y. Li, Y. Li, P. Li, B. Fang, X. Yang, Y. Wen, D.-x. Zheng, C. Zhang, X. He, A. Manchon, Z.-H. Cheng, and X. Zhang, Nonreciprocal charge transport up to room temperature in bulk rashba semiconductor α -GeTe, *Nat. Commun.* **12**, 540 (2021).
- [12] A. Pan and D. C. Marinescu, Nonlinear spin-current generation in quantum wells with arbitrary Rashba-Dresselhaus spin-orbit interactions, *Phys. Rev. B* **99**, 245204 (2019).
- [13] N. W. Ashcroft and N. D. Mermin, *Solid State Physics* (Cengage Learning, Boston, 1976).
- [14] H. Yu, Y. Wu, G.-B. Liu, X. Xu, and W. Yao, Nonlinear Valley and Spin Currents from Fermi Pocket Anisotropy in 2D Crystals, *Phys. Rev. Lett.* **113**, 156603 (2014).
- [15] K. Hamamoto, M. Ezawa, K. W. Kim, T. Morimoto, and N. Nagaosa, Nonlinear spin current generation in noncentrosymmetric spin-orbit coupled systems, *Phys. Rev. B* **95**, 224430 (2017).
- [16] S. Verma, T. Biswas, and T. K. Ghosh, Thermoelectric and optical probes for a Fermi surface topology change in noncentrosymmetric metals, *Phys. Rev. B* **100**, 045201 (2019).
- [17] P. Kapri, B. Dey, and T. K. Ghosh, Role of Berry curvature in the generation of spin currents in Rashba systems, *Phys. Rev. B* **103**, 165401 (2021).
- [18] T. Ideue, L. Ye, J. G. Checkelsky, H. Murakawa, Y. Kaneko, and Y. Tokura, Thermoelectric probe for Fermi surface topology in the three-dimensional Rashba semiconductor BiTeI, *Phys. Rev. B* **92**, 115144 (2015).